Journal of Steroid Biochemistry and Molecular Biology 182 (2018) 72–80

Contents lists available at ScienceDirect

Journal of Steroid Biochemistry and Molecular Biology

journal homepage: www.elsevier.com/locate/jsbmb

Structure and dynamics of neurosteroid binding to the $\alpha_1\beta_2\gamma_2$ $GABA_A$ receptor

Lautaro D. Alvarez[a,c,*], Adali Pecci[b,d]

[a] Universidad de Buenos Aires, Facultad de Ciencias Exactas y Naturales, Departamento de Química Orgánica, Buenos Aires, Argentina
[b] Universidad de Buenos Aires, Facultad de Ciencias Exactas y Naturales, Departamento de Química Biológica, Buenos Aires, Argentina
[c] CONICET – Universidad de Buenos Aires, UMYMFOR, Buenos Aires, Argentina
[d] CONICET – Universidad de Buenos Aires, IFIBYNE, Buenos Aires, Argentina

ARTICLE INFO

Keywords:
$GABA_A$ receptors
Neurosteroids
$\alpha_1\beta_2\gamma_2$ heteropentamer
Binding sites
Docking, molecular dynamics simulation
Potentiation
Activation

ABSTRACT

Neurosteroids are the principal endogenous modulators of the γ-Aminobutyric acid receptors ($GABA_A$Rs), pentameric membrane-bound proteins that can be assembled from at least 19 subunits. In the most abundant $GABA_A$R arrangement ($\alpha_1\beta_2\gamma_2$), neurosteroids can potentiate the GABA action as well as produce a direct activation of the channel. The recent crystal structures of neurosteroids bound to α homopentameric $GABA_A$R reveal binding to five equivalent sites. However, these results have been obtained using receptors that are not physiologically relevant, suggesting a need to investigate neurosteroid binding to heteropentameric receptors that exist in the central nervous system. In a previous work, we predicted the neurosteroid binding site by applying molecular modeling methods on the β_3 homopentamer. Here we construct a homology model of the transmembrane domain of the heteropentameric $\alpha_1\beta_2\gamma_2$ receptor and then, by combining docking and molecular dynamics simulations, we analyzed neurosteroid binding. Results show that the five neurosteroid cavities are conserved in the $\alpha_1\beta_2\gamma_2$ receptor and all of them are able to bind neurosteroids. Two different binding modes were detected depending on the identity of the residue at position 241 in the transmembrane helix 1. These theoretical findings provide microscopic insights into neurosteroid binding at the heteropentameric $GABA_A$R. The existence of two classes of sites may be associated with how neurosteroids modulate $GABA_A$R. Our finding would represent the essential first step to reach a comprehensive understanding of how these endogenous molecules regulate the central nervous system.

1. Introduction

Neurosteroids (NSs) are the principal endogenous modulators of γ-Aminobutyric acid (GABA) action, the major inhibitory neurotransmitter in vertebrate central nervous system (CNS) [1]. GABA is involved in practically all neuronal circuits, modulating functions of critical physiological relevance. Thus central roles in cognition, learning and memory, as well as in anxiety, schizophrenia and epilepsy, among other diseases have been related to alterations in the GABA signaling. Endogenous NS like pregnanolone and allopregnanolone exhibit clear behavioral effects such us anxiolysis, sedation, analgesia, anticonvulsant and anesthesia [2–4]. In this sense, a considerable body of evidence has been accumulated supporting the potential beneficial action of the pharmacological use of NS for the treatment of a great number of disorders. Therefore, the precise knowledge of the molecular basis of action is essential to reach a comprehensive understanding of how these endogenous molecules regulate the CNS.

GABA exerts its action primarily by activating the Gamma-Aminobutyric Acid type A Receptors ($GABA_A$Rs), pentameric membrane-bound proteins belonging to the Cys-loop superfamily of ligand-gated ion channels [5–8]. In mammalians, they potentially assemble from at least 19 subunits belonging to eight different classes ($\alpha_{1\text{-}6}$, $\beta_{1\text{-}3}$, $\gamma_{1\text{-}3}$, δ_1, ε_1, φ_1, π_1 and $\rho_{1\text{-}3}$). Depending on their subunit composition, receptors exhibit distinct pharmacological properties [8]. α_1 is the most abundant subunit in the brain, about 70–90% of all $GABA_A$Rs receptors seem to contain this subunit. The γ2 and β2 subunits are also quite abundant and are present in 50–70% of all $GABA_A$Rs. It is considered that direct synaptic transmissions are mainly mediated by receptors composed by αβγ subunits in the ratio 2:2:1, with an α-β-γ-α-β arrangement (clockwise from the extracellular surface) [7]. Although α or β homopentamers have not been identified in the CNS, they have the ability to form functional channels in vitro that can be allosterically

* Corresponding author at: Departamento de Química Orgánica and UMYMFOR (CONICET-UBA), Facultad de Ciencias Exactas y Naturales, Universidad de Buenos Aires, Pabellón 2, Ciudad Universitaria, C1428EGA Ciudad de Buenos Aires, Argentina.
E-mail address: lalvarez@qo.fcen.uba.ar (L.D. Alvarez).

https://doi.org/10.1016/j.jsbmb.2018.04.012
Received 5 March 2018; Received in revised form 17 April 2018; Accepted 23 April 2018
Available online 26 April 2018
0960-0760/

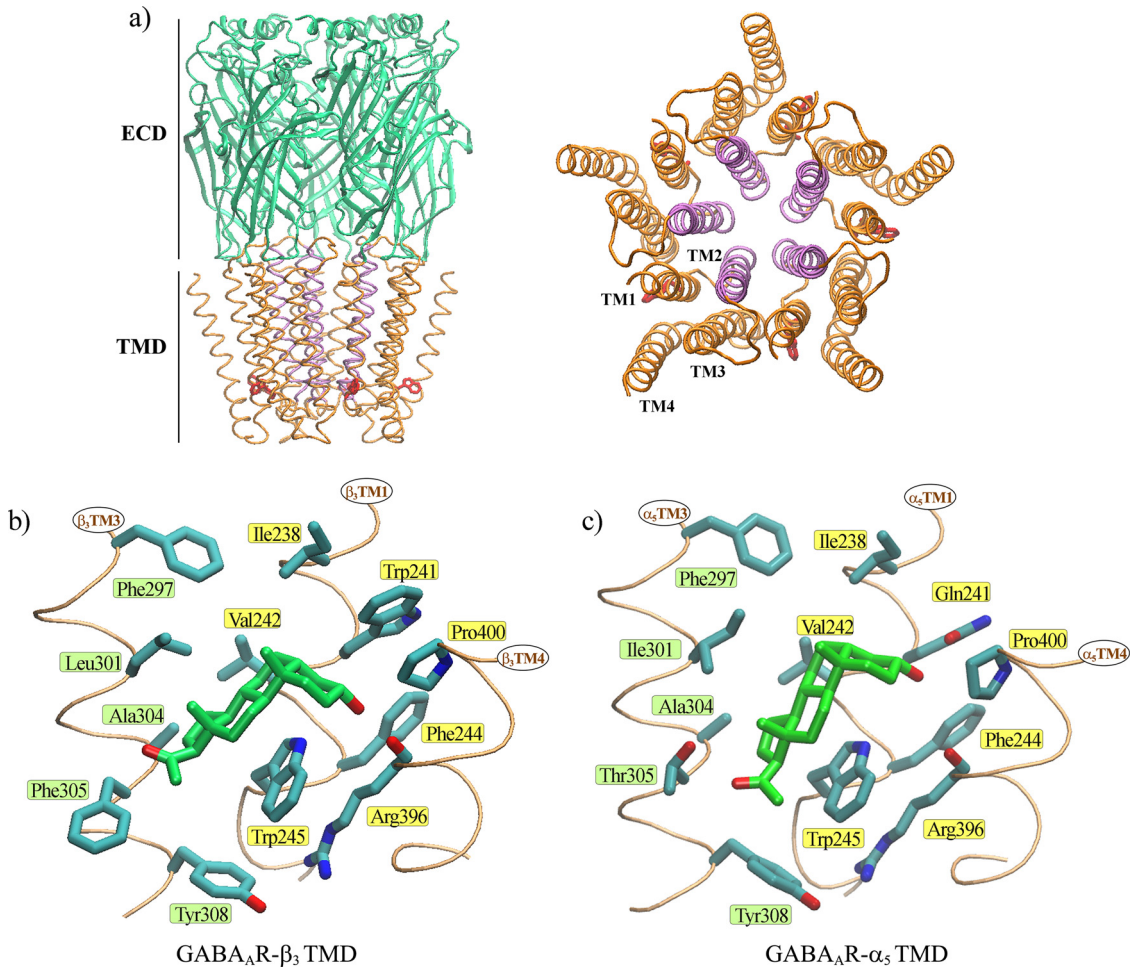

Fig. 1. $GABA_AR$-β_3 accommodates pregnanolone molecules in the transmembrane domain. a) Left panel: lateral view of the $GABA_AR$-β_3 crystal structure (PDB ID: 4COF) showing the extra cellular (ECD) and the transmembrane (TMD) domains. Right panel: view of the TMD from the extracellular space showing the localization of the TM α-helices (TM1-TM4). The Trp245 delimiting the NS cavities are showed in red. b) Detailed view of the pregnanolone binding mode into the $GABA_AR$-β_3 obtained by using molecular modeling tools (Ref. [12]). c) Detailed view of the pregnanolone binding mode observed in the crystal structure of the α_5 TMD (PDB ID: 5O8F) (For interpretation of the references to colour in this figure legend, the reader is referred to the web version of this article).

modulated by NS [9].

Each $GABA_AR$ subunit is composed by three domains: the extracellular domain (ECD), the transmembrane domain (TMD) formed by four α-helices (TM1–TM4), and a cytoplasmic loop of variable length (Fig. 1a). Subunits assembly creates a central ion conducting pore that allows the flux of chloride ions from the extracellular to the intracellular compartment. The five TM2 segments of the pentameric receptor constitute the ion channel. These segments are surrounded by TM1 and TM3 α-helices, shielding TM2 residues from the membrane. Residues from TM1 and TM3 α-helices participate in the inter-subunit interactions, while TM4 helices are located at the periphery of the channel. GABA binds to an orthosteric site (the GABA-binding pocket) that localizes in the α/β extracellular interface [7]. Other allosteric sites are present in the $GABA_ARs$, such as those interacting with numerous clinically well used compounds, like benzodiazepines, etomidate and propofol, which upon binding modulate the conformational state of the receptor [7]. It is well know that in the $\alpha_1\beta_2\gamma_2$ receptor arrangement, NS can either potentiate the chloride current elicited by GABA (at nanomolar concentration) or directly activate the receptor in the absent of the neurotransmitter (at micromolar concentration). On this basis, Hosie et al have initially proposed that two different NS binding sites would be present in the $GABA_AR$-$\alpha_1\beta_2\gamma_2$: an activation and a potentiation sites [10,11]. The presence of an α subunits is essential to the potentiation action of NS.

The resolution of the first $GABA_AR$ X-ray structure [13], the $GABA_AR$ homopentamer composed by β_3 subunits ($GABA_AR$-β_3), has represented a great advance for the study of the NS/$GABA_AR$ binding. In a previous work we reported the presence of five cavities in the $GABA_AR$-β_3 TMD crystal structure, which are located between the TM3 of one subunit and the TM1 of the adjacent one [12]. By using a combination of molecular modeling tools (docking and molecular dynamics (MD) simulation), we have shown for the first time that these cavities can accommodate pregnanolone (Fig. 1b) and allopregnanolone in a proper and specific manner. Notably, the recent resolution of the X-ray structures of $GABA_AR$ chimeras of α_1 or α_5 homopentamers [14,15] in which NS are co-crystallized at the TMD, have strongly confirmed our previous molecular modeling predictions (Fig. 1c). The localization of the site as well as the orientation acquired by the steroid are practically identical between the experimental and the simulation results.

In view of the accurate predictions obtained by the molecular modeling, here we constructed a homology model of the $GABA_AR$-$\alpha_1\beta_2\gamma_2$ and studied the molecular basis of the NS binding at the more abundant and physiologically relevant $GABA_A$-R arrangement existing in the CNS.

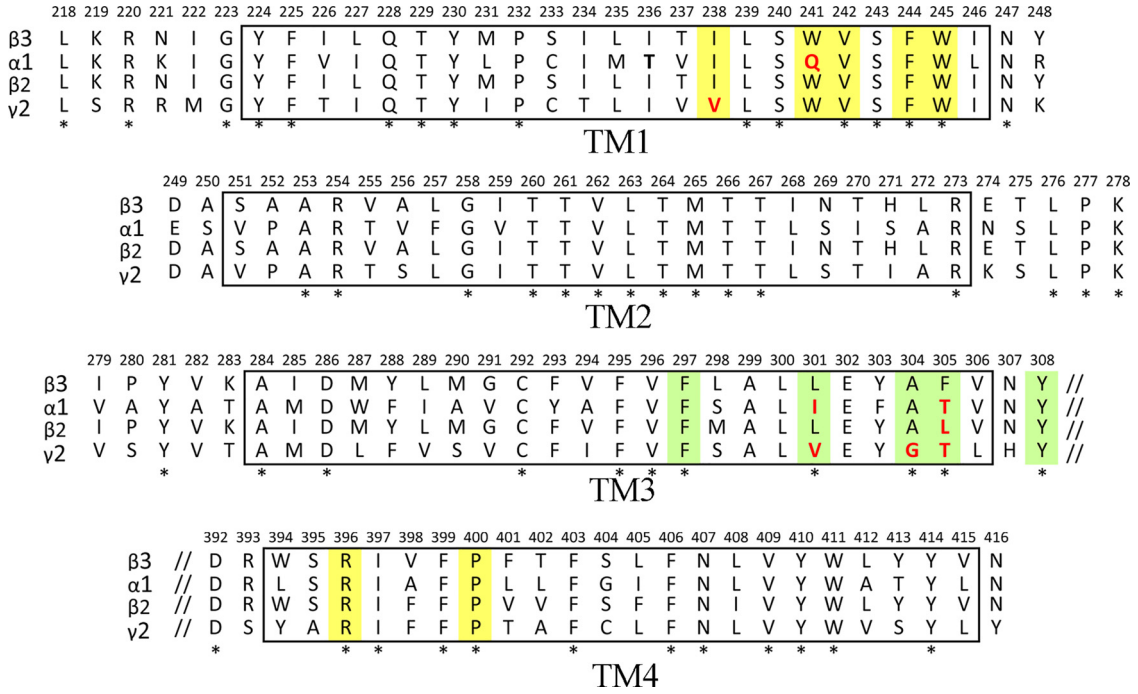

Fig. 2. The sequence alignment of $GABA_A$ subunits reveals that the majority of NS binding site residues are conserved. Sequence alignment of the human α_1, β_2, β_3 and γ_2 $GABA_A$ subunits. Conserved residues are indicated with an asterisk. Residues forming the NS binding sites are highlighted (the TM1 and TM4 residues of one subunit in yellow and the TM3 residues of the adjacent subunit in green). For comparison purposes, the numbering utilized by Hosie et al [10], corresponding to the mouse α_1 mature protein, was used for all the $GABA_A$ subunits (For interpretation of the references to colour in this figure legend, the reader is referred to the web version of this article).

2. Results and discussion

2.1. Construction of the $GABA_AR$-$\alpha_1\beta_2\gamma_2$ TMD model

X rays structures and molecular modeling have shown that the residues constituting the neurosteroid binding sites are located near the intracellular side of the receptor [12,14,15]. The cavities are formed by five residues of the TM1 C terminal end together with two residues from the TM4 C-terminal end (Fig. 2, residues highlighted in yellow) and four residues from the TM3 N-terminal end of the adjacent subunit (Fig. 2, residues highlighted in green). In contrast to homopentameric receptors, where the five cavities are equivalent, the subunits arrangement of $GABA_AR$-$\alpha_1\beta_2\gamma_2$ conforms four different interfaces with four different NS binding pockets (Fig. 3a). The alignment of the β_3 TMD sequence with the α_1, β_2, and γ_2 sequences shows that the majority of NS binding site residues are conserved or are replaced by amino acids with similar chemical properties (Fig. 2). Relevant substitutions are present at position 241 (Gln in α_1 compared with the Trp in the other subunits) and at position 305 (Phe in β_3 is substituted by a Thr in α_1 and γ_2 subunits or by a Leu in β_2). In view of these small differences, no great structural changes should be expected in the global constitution of NS binding sites of the heteropentameric receptor.

The $GABA_AR$-$\alpha_1\beta_2\gamma_2$ TMD model was constructed using the Modeller program [16] and the $GABA_AR$-β_3 TMD as template structure (PDB ID: 4COF). Twenty homology models were obtained, and then the best ranked was energetically minimized to obtain the initial model. A comparative analysis between the constructed $GABA_AR$-$\alpha_1\beta_2\gamma_2$ and the $GABA_AR$-β_3 crystal structure reveals that at least one residue differs between both structures in each NS cavity (Fig. 3b). Two replacements occur for cavities I and IV: β_3Trp241 and β_3Phe305 by α_1Gln241 and β_2Leu305, respectively. As a result, the volume of these cavities decreases (Table 1). Oppositely, the replacement of β_3Ala304 and β_3Phe305 by γ_2Gly304 and γ_2Thr305, respectively, produces a large increase in the volume of cavity II. The replacement of three residues in cavity III, β_3Ile238, β_3Leu301, β_3Phe305 by γ_2Val238, α_1Ile301 and α_1Thr305 results in a slightly reduction of the volume. Finally, only one residue differs in the cavity V: β_3Phe305 by α_1Thr305. In the $GABA_AR$-β_3 crystal structure, the β_3Trp245 of cavity V presents an alternative conformation. When χ_1 and χ_2 torsion angles of the Trp245 were rotated in a way to obtain a conformation similar to that observed in the other cavities, volumes of cavity V of both homopentameric and heteropentameric systems were similar.

The above preliminary findings indicate a high structural similarity among the NS cavities in the $GABA_AR$-$\alpha_1\beta_2\gamma_2$ model. Moreover, all of them appear to be large enough to accommodate a NS molecule.

2.2. MD simulation of the apo $GABA_AR$-$\alpha_1\beta_2\gamma_2$

Once the initial $GABA_AR$-$\alpha_1\beta_2\gamma_2$ model was constructed, we carried out MD simulations of the apo receptor immersed in a lipidic membrane model composed by 1-Palmitoyl-2-Oleoyl-sn-Glycero-3-Phosphatidylcholine (POPC) molecules. Three independent 100 ns production runs (1–3) were obtained. In all of them the overall structure of the receptor was well conserved, with the RMSD values measured over the backbone atoms converging to ca 2.5 Å (Fig. 4a). Regarding to the NS cavities, the visual inspection of the trajectories revealed that each one can evolve to two possible states: expanded or collapsed. The Fig. 4b shows a representative snapshot of the cavity I in the expanded state. The residues conserve their disposition while the lipid molecules fill the cavities, forming an extensive contact with the hydrophobic residues, especially with the planar surface of the Trp245 side chain. Oppositely, in the collapsed state (Fig. 4c), residues move to form protein-protein interactions excluding lipid molecules from the cavity.

In order to determine the number of lipids atoms inside the cavities, we calculated the radial distribution function (RDF) of the POPC atoms using the Val242 side chain as center of mass (Fig. 4d). This residue was selected due to its position in the deepest region of the pocket. We found that cavities in an expanded state correspond to RDF curves with a maximal value between 5 and 6 Å. We concluded that almost half of

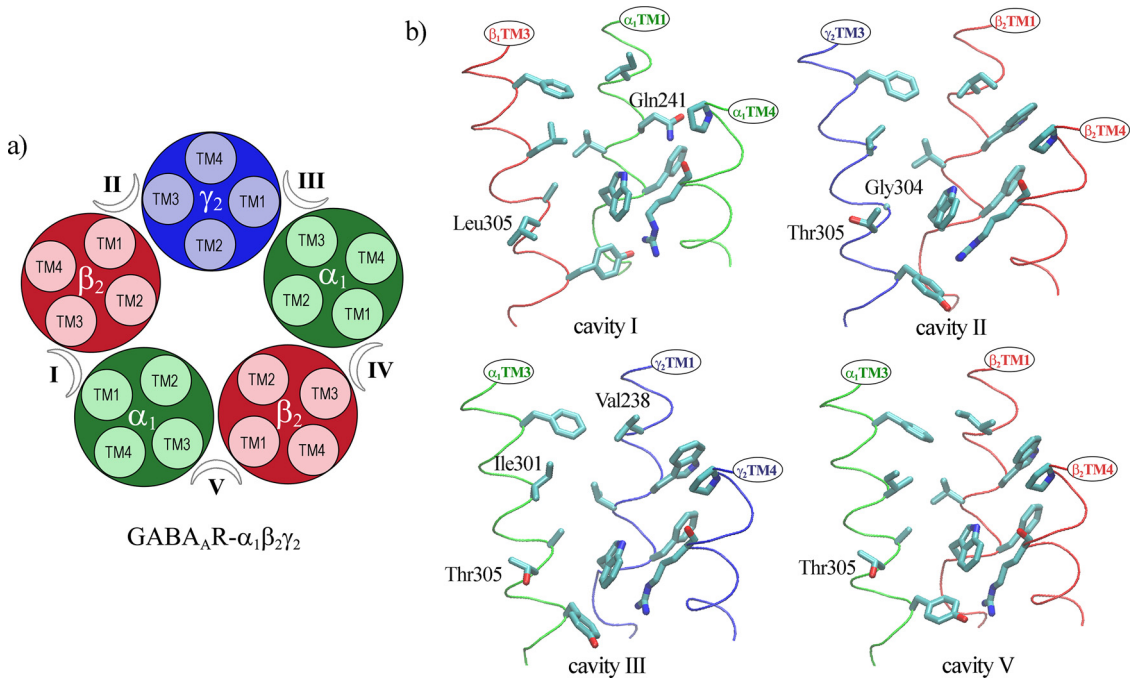

Fig. 3. The heteropentameric receptor model reveals four structurally similar NS cavities. a) Schematic representation of the $GABA_AR$-$\alpha_1\beta_2\gamma_2$ TMD. b) Neurosteroid cavities in the initial model of the apo $GABA_AR$-$\alpha_1\beta_2\gamma_2$. The names of residues that changes respect to the $GABA_AR$-β_3 cavities are indicated. Cavity IV is equivalent to cavity I.

the cavities (8 of 15) evolved to an expanded state (cavities I, II and V in run 1; I, IV and V in run 2 and III and V in run 3). Moreover, each cavity evolved to an expanded state in at least one MD run, indicating that all of them have the ability to contain hydrophobic lipid chains.

In summary, by simulating the apo $GABA_AR$-$\alpha_1\beta_2\gamma_2$ system we found that in those NS cavities where POPC molecules fill the free spaces, the expanded conformation remains stable and the global shape of the pocket is conserved.

2.3. Docking of pregnanolone

As a first approach to investigate the NS binding mode in cavities I–+V of the $GABA_AR$-$\alpha_1\beta_2\gamma_2$ model, we used the Autodock4 program [17] to dock pregnanolone into the initial coordinates. Grids centered in the geometrical center among residues forming the cavity were constructed and then, 500 runs of genetic algorithm were analyzed with a cluster tolerance of 2 Å. Although variable frequencies and energies were obtained (Table 1), a pose similar to the that experimentally observed [15]-and similar to the obtained by the application of molecular modeling tools on the $GABA_AR$-β_3 structure [12]- was always the most favored pose for all cavities. Remarkably, despite the polar interaction formed between the 3α-OH of the NS and the α_1Gln241, cavities I and IV exhibited the lowest favorable energies and poorest frequencies. We then selected snapshots at 50 and 100 ns from the apo MD runs, deleted the lipid molecules from the expanded state cavities and docked the pregnanolone molecule. Again, the above pose was the most favored in all cases, reaching frequencies around 50% (Table 1). Compared to the results obtained using the initial model, a clear increase of the cluster

Table 1
Volume, docking and energy contributions of neurosteroid binding.

		Cavity				
		I	II	III	IV	V
Volume (Å^3)[a]		339 (498)	734 (552)	568 (591)	321 (527)	670 (669)
Docking (Kcal/mol)[b]						
Initial Model		−5.1 (27)	−6.9 (65)	−6.6 (75)	−5.4 (30)	−7.1 (42)
MD run1	50 ns	−5.8 (51)	−6.2 (35)	nd	nd	−5.8 (55)
	100 ns	−5.8 (56)	−6.1 (27)	nd	nd	−5.8 (53)
MD run 2	50 ns	−5.9 (55)	nd	nd	−5.7 (48)	−6.1 (46)
	100 ns	−6.1 (53)	nd	nd	−5.8 (52)	−6.1 (49)
MD run 3	50 ns	nd	nd	−6.4 (54)	nd	−6.6 (47)
	100 ns	nd	nd	−6.2 (58)	nd	−6.6 (44)
MM/PBSA (Kcal/mol)[c]						
Ele		−11.8	−12.0	−12.0	−11.2	−11.8
Vdw		−48.5	−48.4	−51.9	−49.2	−52.2

[a] Volume of NS cavities of the $GABA_AR$-$\alpha_1\beta_2\gamma_2$ initial model calculated with the fpocket program. The values between parentheses correspond to the volumes calculated for the $GABA_AR$-β_3 crystal structure.

[b] Lowest binding Autodock energies of pregnanolone in the $GABA_AR$-$\alpha_1\beta_2\gamma_2$ system. The values between parentheses correspond to the frequencies observed for each cluster.

[c] Ligand-receptor energy contributions to the total energy of the MM force field computed using the MM/PBSA method (vdw: Van der Waals; Ele: electrostatic). The PBSA terms were ignored. nd: not determined.

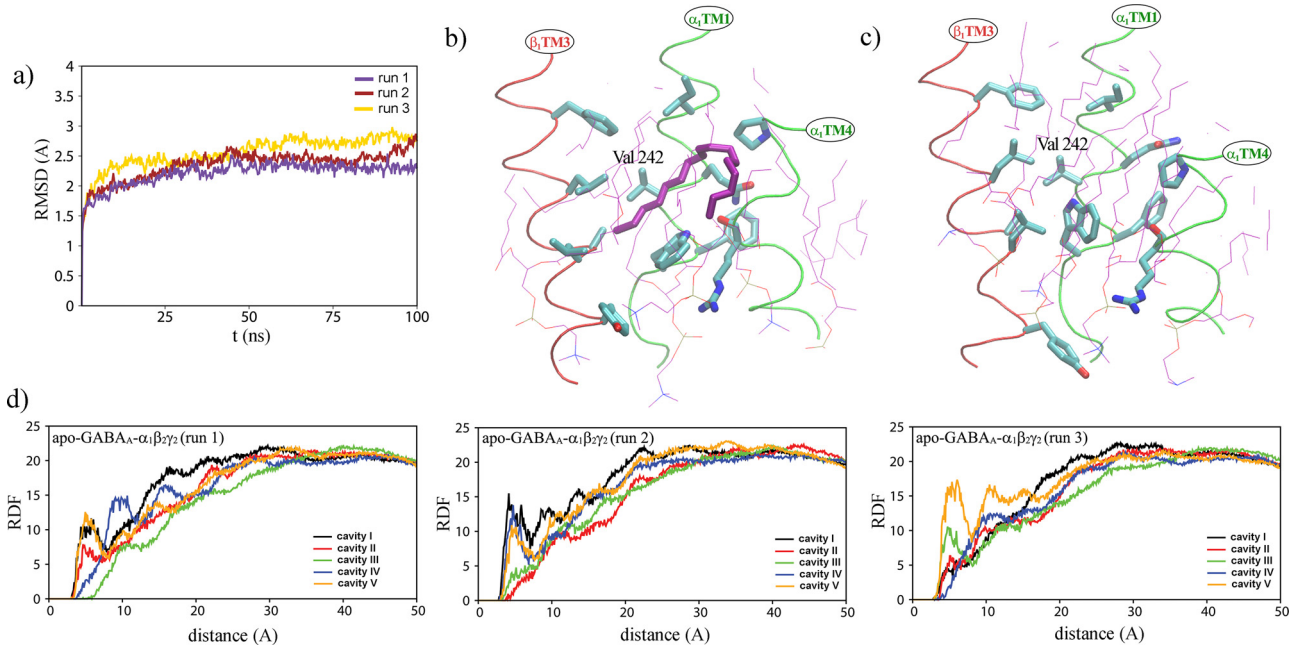

Fig. 4. Apo MD simulation reveals two alternative states of the NS cavities (expanded or collapsed). a) RMSD measured over CA atoms of the apo $GABA_AR$-$\alpha_1\beta_2\gamma_2\beta_3$ system (run 1 in purple, run 2 in brown and run 3 in yellow). b) Representative snapshot of the cavity I of the apo $GABA_AR$-$\alpha_1\beta_2\gamma_2\beta_3$ TMD system (run 1) in the expanded state. POPC palmitoyl chain inside of the cavity is showed in purple. c) Representative snapshot of the cavity IV of the apo $GABA_AR$-$\alpha_1\beta_2\gamma_2\beta_3$ TMD system (run 1) in the collapsed state. d) Radial distribution function (RDF, arbitrary units) of the POPC atoms using the Val242 side chain as geometric center. Values of the cavities I (black), II (red), III (green), IV (blue) and V (orange) are showed for the three independent MD runs (For interpretation of the references to colour in this figure legend, the reader is referred to the web version of this article).

frequency together with a reduction of the docking energies were observed in cavities I and IV, indicating that protein stabilization improved NS binding to these sites.

Thus, docking results reveal that the five cavities of the $GABA_AR$-$\alpha_1\beta_2\gamma_2$ have the ability to accommodate steroidal molecules with a preferential binding orientation.

2.4. MD simulation of the holo $GABA_AR$-$\alpha_1\beta_2\gamma_2$ systems

2.4.1. Binding mode of pregnanolone

In order to further evaluate the dynamics of the binding between pregnanolone and the receptor, we constructed a $GABA_AR$-$\alpha_1\beta_2\gamma_2$ system with five ligands, one in each NS cavity I–V. Ligand coordinates were obtained from the best docking solution in the initial model. The complex was immersed in a POPC membrane model and 200 ns of MD simulation were obtained (coordinates of the final stabilized $GABA_AR$-$\alpha_1\beta_2\gamma_2$ /pregnanolone complex are detailed in Supporting Information). The RMSD of backbone atoms reveals a stabilized receptor structure (Fig. 5a) while all pregnanolone molecules, after an initial arrangement, reached a tightly binding mode (Fig. 5b) very close to the original one. The stacking between the B, C and D steroid rings and the aromatic side chain of the TM1 Trp245, and the formation of two specific ligand-receptor hydrogen bonds are the main characteristic of the NS-receptor interaction (Fig. 6a). Except for cavity II, the time evolution of the angle formed between the normal to the plane of the steroidal skeleton (determined by C6, C10 and C13 atoms) and the normal to the plane of the Trp245 indole ring (determined by CD1, CZ2 and CE3 atoms) reveals a stable almost parallel disposition between the steroid and the Trp in all cavities. (Fig. 5c). Notably, the observed values are very close to those calculated in the crystal structure of the α_5 homopentamer (1.7–4,3°). To further investigate the binding in the cavity II, an additional MD simulation was performed using the coordinates obtained when the pregnanolone was docked in the 50 ns snapshot of the apo $GABA_AR$-$\alpha_1\beta_2\gamma_2$ model (run 1). In this trajectory, a tightly binding mode was observed, very similar to the obtained for the other cavities (data not shown).

Regarding the polar contacts, a hydrogen bond is formed between the oxygen atom of the steroid 3α-OH moiety and the nitrogen atom of the TM1 Trp245 side chain in all the cavities (Distance A, Fig.6b). A second hydrogen bond, formed by the 3α-OH, depended on the TM1 cavity identity. As it was observed for the $GABA_AR$-β_3 system, in cavities II, III and V the 3α−OH group works as a donor, sharing its hydrogen with the oxygen backbone atom of the Arg396 (Distance C, Fig. 6b). This interaction was clearly more persistent for cavity III. In contrast, in cavities I and IV this interaction is replaced by the formation of a hydrogen bond with the oxygen atom of α_1Gln241 side chain (Distance B, Fig. 6b). Thus, a clear difference in the recognition of the 3α-OH can be detected among cavities with a Trp (II, III and V) or a Gln (I and IV) at position 241. At the same time, different relative orientations of the steroid in respect to the membrane can be distinguished between the two type of cavities (Fig. 5d). Remarkably, the values obtained for cavities I and IV fluctuate around those calculated from the crystal structure of the α_5 homopentamer/pregnanolone complex (PDB ID: 5O8F) (110.0–113.1°).

On the other hand, although the steroidal side chain conserves the original conformation during the 200 ns, the C20 carbonyl group does not form direct polar interactions with the receptor residues. Even in those cavities where the Thr305 is close to the steroidal D-ring (cavities II, III and V), no direct interactions among these polar moieties were observed. Instead, the Thr305 is strongly anchored to the protein, forming a hydrogen bond with the oxygen backbone atom of the residue at position 301 (Distance D, Fig. 6b). From the crystal structure of the α_5 homopentamer/pregnanolone complex it was proposed that the C20 carbonyl group forms a hydrogen bond with the α_5Thr305. However, a detailed analysis of this structure reveals that the oxygen atom of the hydroxyl group of Thr305 is closer to the oxygen backbone atom of the Ile301 (2,8 Å averaging all the cavities) rather the C20-carbonyl oxygen atom (3.3 Å averaging all the cavities). This suggests that the Thr305 side chain forms a protein-protein and not a protein-ligand hydrogen bond, as it was observed by MD simulation.

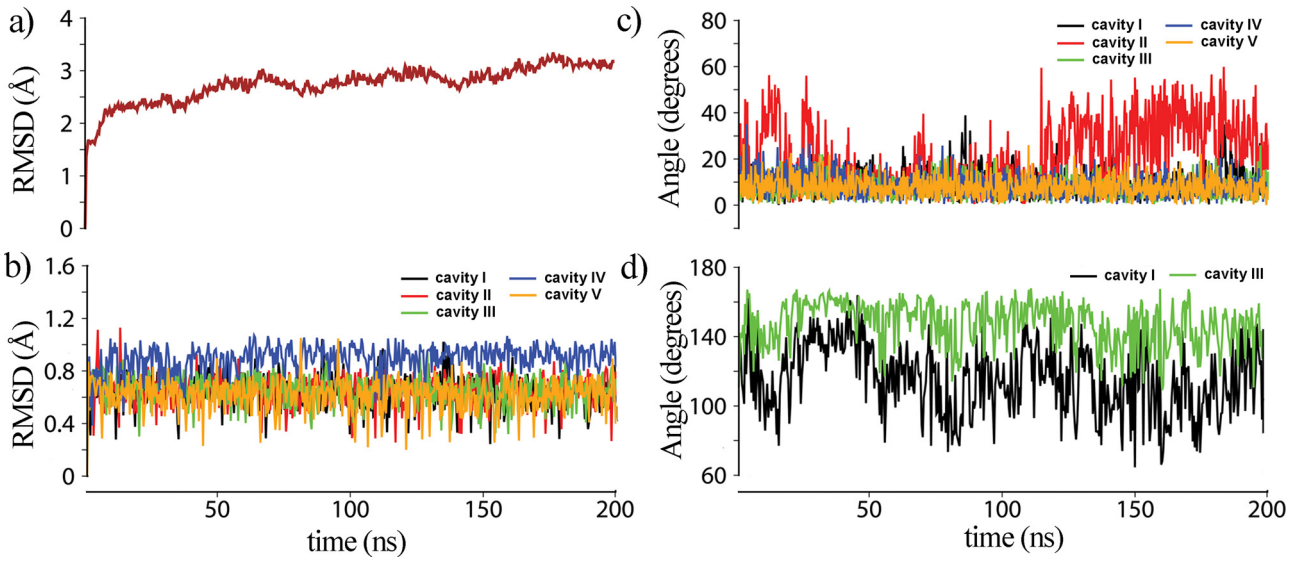

Fig. 5. Pregnanolone reaches a tightly binding mode in the MD simulation. a) RMSD measured over CA atoms of the holo $GABA_AR$-$\alpha_1\beta_2\gamma_2$/pregnanolone system. b) RMSD measured over carbon atoms of the pregnanolone steroidal skeleton in cavities I (black), II (red), III (green), IV (blue) and V (orange). c) Time evolution of the angle formed between the normal to the plane of the steroid and the normal to the plane of the Trp245 indole ring in cavities I (black), II (red), III (green), IV (blue) and V (orange). d) Time evolution of the angle formed between the normal to the plane of the steroid and the z-axis in cavities I (black) and III (green) (For interpretation of the references to colour in this figure legend, the reader is referred to the web version of this article).

Finally, in order to estimate the energetic contributions from the electrostatic energy and Van der Waals interactions, the sum of which gave the total molecular mechanics (MM) binding energy, we used the MM/PBSA method [18]. No significant differences were founded among cavities (Table 1). In all cases the NS binding is mainly governed by the hydrophobic contacts. The electrostatic contributions were similar for those sites in which the 3α-OH interacts with the Gln241 and in those sites where the hydrogen bond is formed with the Arg396. These results suggest that the affinity of pregnanolone could be similar for all cavities.

2.4.2. *Binding mode of allopregnanolone*

Next we investigated the binding mode of the 5α isomer of pregnanolone (allopregnanolone), which has an overall flat structure. Allopregnenolone was docked in cavity I of the initial $GABA_AR$-$\alpha_1\beta_2\gamma_2$ model and then the complex was MD simulated by 100 ns. Previous results obtained with the $GABA_AR$-β_3 system have shown that its NS cavities are able to specifically recognize the allopreganolone [12]. Here, docking and MD results confirmed that allopregnanolone can also be recognized by cavities where a Gln occupies the position 241. The hydrogen bonds described for pregnanolone binding are also stably observed with the flat isomer. Fig. 7 shows a representative snapshot of allopregnanolone in cavity I, where a parallel disposition between the

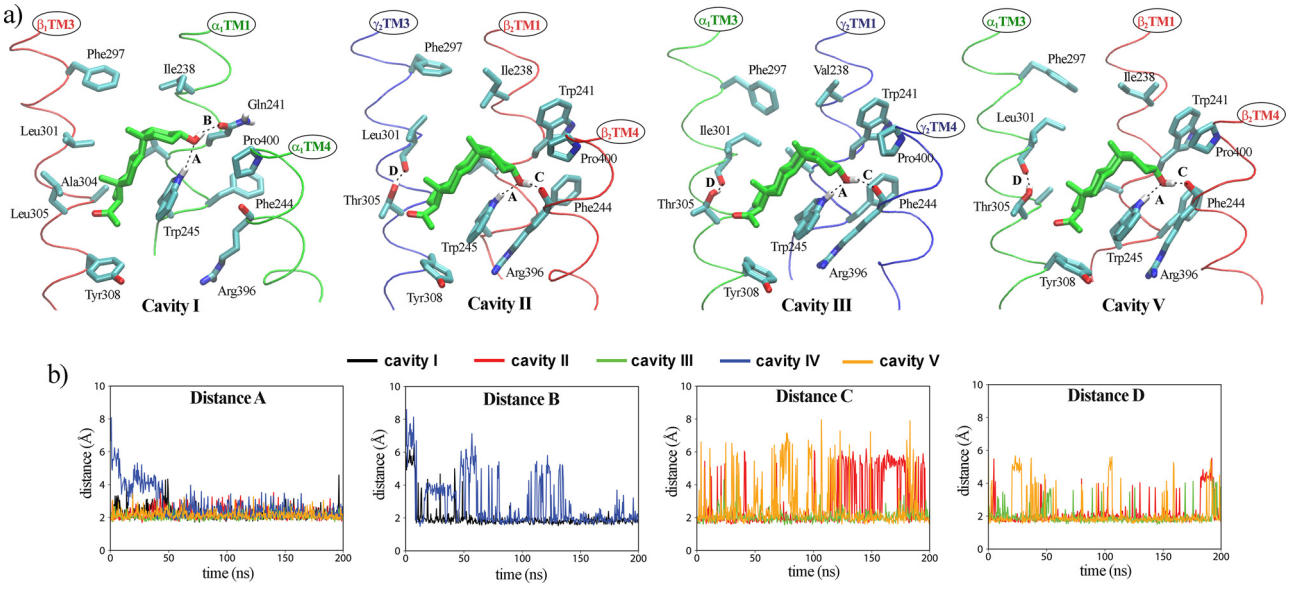

Fig. 6. Specific hydrogen bonds anchor pregnanolobne C3-hydroxyl. a) Representative snapshots of the pregnanolone binding mode in cavities I, II, III and V of the $GABA_AR$-$\alpha_1\beta_2\gamma_2$ system. b) Time evolution of the distances between the pregnanolone C3-hydroxyl oxygen atom and the Trp245 HE1 atom (Distance A), the pregnanolone C3-hydroxyl hydrogen atom and the Gln241 OE1 atom (Distance B), the pregnanolone C3-hydroxyl hydrogen atom and the Arg396 oxygen backbone atom (Distance C) and, the Thr305 HG1 atom and the Leu/Ile301 oxygen backbone atom (Distance D). Cavities I (black), II (red), III (green), IV (blue) and V (orange) (For interpretation of the references to colour in this figure legend, the reader is referred to the web version of this article).

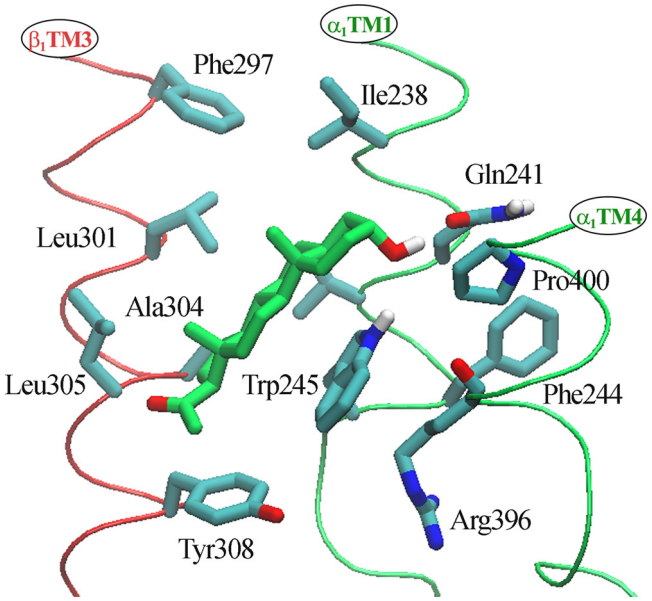

Fig. 7. Cavity I accommodates allopregnanolone. Representative snapshot of the allopregnanolone binding mode in the cavity I of the GABA$_A$R-$\alpha_1\beta_2\gamma_2$ system.

planar structure of the rings scaffold and the α_1Trp245 indole group is established. Remarkably, a similar disposition was found in the crystal structure of the α_1 homopentamer TMD bound to tetrahydro-deoxycorticosterone [14]. Furthermore, the MM/PBSA method was used to estimate the energy of the allopregnanolone-receptor interaction, finding very similar values to those calculated for pregnanolone in the same cavity.

2.4.3. Role of the α_1Gln241

As was mentioned above, neurosteroid potentiation is dependent on the presence of α subunits, which contribute the conserved αGln241. When this residue is mutated to hydrophobic amino acids, the ability of NS to potentiate GABA function is lost [10,19]. To gain insight in the role played by the α_1Gln241, we compared the hydrogen bond network formed in cavity I in the presence of POPC or in the presence of pregnanolone (apo run 1 and holo systems, respectively). In the absence of pregnanolone, α_1Trp245 and α_1Gln241 maintain hydrogen bonds with their neighbor residues (Fig. 8a). While the nitrogen atom of the α_1Trp245 indole ring interacts with the oxygen backbone atom of α_1Arg396, the α_1Gln241 side chain forms three hydrogen bonds: two of them throughout the nitrogen atom (one with the proper α_1Gln241 oxygen backbone atom and the other with the α_1Ser107 oxygen backbone atom) and the third one between the oxygen atom and the α_1Phe111 nitrogen backbone atom. As consequence of the formation of this hydrogen bonding network, a direct interaction among TM1 and TM4 residues is stablished.

When pregnanolone occupies the cavity I, a deep restructuration of hydrogen bonds involving α_1Trp245 and α_1Gln241 is produced (Fig. 8b). To contact the steroid, these residues interact with each other throughout their backbone atoms, while the nitrogen atom of the amide of the α_1Gln241 is located pointing towards a hydrophobic region. In this way, we found that the presence of pregnanolone impedes the formation of the hydrogen bonding network between TM1-TM4 at this region of the TMD. Oppositely, in the cavities II, III and V, where a Trp occupies the position 241 (Fig. 8c), the steroidal 3α-OH group works as a bridge between the these α-helices, connecting them through the formation of hydrogen bonds with Trp245 (TM1) and Arg396 (TM4).

3. Conclusion

Until recently, the lack of X-ray structures of GABA$_A$Rs have precluded the acquisition of precise information on the NS binding mode. Despite the fact that Hosie et al built the GABA$_A$R TMD model starting with a dissimilar template (the acetylcholine receptor) [10], it was for years the more accepted model in the community. However, new biochemical data and the recent resolution of two GABA$_A$R/NS crystal structures revealed that this model is basically incorrect, although it predicted the relevance of the α_1Gln241 for NS recognition. Auspiciously, we have previously showed that the application of molecular modeling tools on the GABA$_A$R-β_3 crystal structure did generate a correct prediction for both the localization and the binding mode of neurosteroids [12].

In this work we propose for the first time a molecular model of the interaction between NS and the main receptor arrangement expressed in the CNS, the GABA$_A$R-$\alpha_1\beta_2\gamma_2$. We found that the five neurosteroid cavities observed in the β_3 and in the α_5 homopentamers are conserved in the heteropentamer. Moreover, all of them were able to bind neurosteroids in a proper manner. Although they are very similar, there are some particular differences that affect how NS are recognized by each cavity. Mainly, we conclude that the identity of the residue located at position 241 determines which hydrogen bonds are formed between the neurosteroid 3α-OH group and the receptor residues. On the other hand, we also noted that in contrast to the α_5 homopentamer, there are no NS cavities containing polar amino acids at both positions 241 and 305 in the heteropentameric receptor. Thus, some differences should be expected between the binding mode observed in the X-rays structure (PDB ID: 5O8F) and the binding mode in the GABA$_A$R-$\alpha_1\beta_2\gamma_2$.

Trp245 works as a planar platform in which the steroid lies its planar scaffold. The fact that all 19 known subunits have a Trp at this TM1 position suggests that any GABA$_A$R should be able, in principle, to bind five NS molecules. However, the functional role of NS cavities in

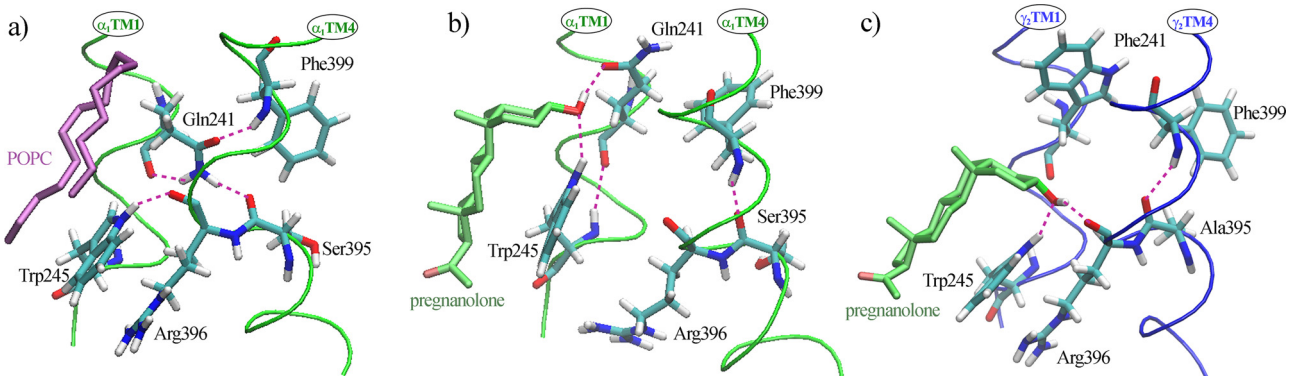

Fig. 8. Pregnanolone affects the TM1-TM4 interaction. Representative snapshots of the apo (a) and holo (b) cavity I and the holo (c) cavity III of the GABA$_A$R-$\alpha_1\beta_2\gamma_2$ systems. The hydrogen bonds formed between αTM1 and αTM4 residues are indicated with dotted lines.

non-alpha $GABA_AR$s is still unclear. For example, in electrophysiological assays performed with $GABA_AR$-β_3, allopreganolone did not activate discernible currents [20]. Nevertheless, neurosteroids do cause a small enhancement of propofol-activated currents and strongly inhibit the [^{35}S]TBPS binding, indicating an allosteric modulation of the $GABA_AR$-β_3 structure. On the other hand, it is well known that the NS potentiation effect is αTM1 dependent mainly due to the presence of Gln241. We found that the NS binding at the αTM1 sites, located at the same interfaces as the GABA binding sites, alters the αTM1-αTM4 interaction. Although further studies using both ECD and TMD should be required to understand the allosteric communication between NS and GABA, our findings suggest that the disruption of the αTM1-αTM4 interaction would be part of the mechanism for which the NS signal is integrated.

To comprehensively decipher the intricate relationships among steroids, protein and membrane, different scenarios should be considered. In this context, we believe that the simpler hypothesis to explain the activation/potentiation effects resides in the occupation degree of the different $GABA_AR$ cavities. At low concentrations the NS may bind either site of the receptor, but when it binds to αTM1 site, the GABA potentiation occurs. At high NS concentrations, all cavities would be occupied provoking the direct channel activation. Although further studies will be necessary to test this proposal, we consider that molecular modeling is a powerful tool that has allow us to gain insights on NS binding at this physiologically relevant $GABA_AR$ that has not yet been crystallized.

4. Computational methods

4.1. Initial $GABA_AR$-$\alpha_1\beta_2\gamma_2$ TMD structure

The initial $GABA_AR$-$\alpha_1\beta_2\gamma_2$ TMD structure was constructed by using the Modeller program [16] and the crystal structure of the $GABA_AR$-β_3 (PDB ID: 4COF) as template. Extracellular domains (residues 1 to 213) were removed from all the subunits and the artificial loops between TM3 and TM4 were conserved as in the crystal structure. Once manually aligned the human α_1 (Uniprot: P14867), β_2 (Uniprot: P47870) and γ_2 (Uniprot: P18507) subunits on the $GABA_AR$-β_3 structure (α_1 with chains A and D, β_2 with chains B and γ_2 with chain C) twenty different models were obtained with the default parameters of Modeller. Then the best ranked structure was energetically minimized in form to obtain the initial coordinates of the $GABA_AR$-$\alpha_1\beta_2\gamma_2$ TMD structure. For comparison purposes, the numbering utilized by Hosie et al [10], corresponding to the mouse α_1 mature protein, was used for all the $GABA_A$ subunits (see Fig. 2). The structures of steroids, pregnanolone (3α-hydroxy-5β-pregnan-20-one) and allopregnanolone (3α-hydroxy-5α-pregnan-20-one), were optimized with the *ab initio* method HF/6-31G** using the Gaussian 03 program [21].

4.2. Docking

The Autodock 4.2 program [17] was used to dock the optimized structures of steroids into the initial $GABA_AR$-$\alpha_1\beta_2\gamma_2$ TMD model or into snapshots extracted from the MD trajectory of the apo system. Rotatable bonds of steroids (C3-O3 and C17-C20) were allowed to rotate freely, while the receptor was considered as a rigid molecule. Five grids (one for each cavity I–V) of 110 × 110 × 110 points with a spacing of 0.2 Å centered in the geometrical center among residues that form the cavities, were calculated and used to obtain 500 runs of the genetic algorithm method. Solutions were analyzed with a cluster tolerance of 2 Å.

4.3. Molecular dynamics simulation

Molecular dynamics simulations (MD) were performed with the AMBER 14 software package [22]. The initial coordinates of the apo $GABA_AR$-$\alpha_1\beta_2\gamma_2$ TMD immersed in a 1-Palmitoyl-2-Oleoyl-sn-Glycero-3-Phosphatidylcholine (POPC) membrane bilayer were obtained with the Membrane Builder utility [23] using the replacement method. The first principal axis of the receptor was aligned to the *z*-axis and then the receptor was embedded into a 125 Å × 125 Å POPC membrane fully hydrated with TIP3P water molecules (thickness of 30 Å on top and bottom of the system). Na^+ and Cl^- were added to obtain a final ion concentration of 0.15 M. The resultant system is composed by one $GABA_AR$-$\alpha_1\beta_2\gamma_2$ TMD, 418 POPC, 110 Cl^- ions, 85 Na^+ ions, and 35,500 water molecules given a total of over 173,000 atoms. The holo system was constructed from the initial apo system using the best docking solution of pregnanolone in each cavity. No superpositions between steroids and POPC molecules were found in this initial system. The FF14SB force field parameters [24] were used for all receptor residues and the Lipid14 force field parameters [25] were used for POPC molecules. Steroid parameters were assigned according to the general AMBER force field (GAFF) [26] and the corresponding RESP charges at the HF/6-31G** level using the Antechamber module.

Systems were initially minimized for 10,000 steps and then were heated through two sequential steps of 250 ps. First, systems were heated to 200 K at constant volume. Then temperature was slowly increased at constant pressure to the desired production temperature (300 K). In both steps a restraint (10 kcal/mol/Å^2) fixing the backbone protein and lipid atoms was applied. Finally, 250 ps were carried out at 1 atm and 300 K in which the restraint on the protein backbone and lipids was gradually reduced to zero. Starting from these equilibrated structures, three independent MD production runs of 100 ns of the apo $GABA_AR$-$\alpha_1\beta_2\gamma_2$ TMD and one MD production runs of 200 ns of the holo $GABA_AR$-$\alpha_1\beta_2\gamma_2$ TMD were carried out. All production simulations were performed at 1 atm and 300 K, maintained with the Berendsen barostat and thermostat respectively, using periodic boundary conditions and the particle mesh Ewald method (grid spacing of 1 Å) for treating long-range electrostatic interactions with a uniform neutralizing plasma. The SHAKE algorithm was used to keep bonds involving H atoms at their equilibrium length, allowing the use of a 2 fs time step for the integration of Newton's equations. In all systems, in order to maintain the overall position of the truncated N-terminal extreme, a small harmonic restraint (with force constant of 3 kcal/mol/Å^2) was applied to CA atoms of the first two N-terminal residues of each subunit.

4.4. Analysis of the results

The fpocket method [27] was applied on the initial model of the $GABA_AR$-$\alpha_1\beta_2\gamma_2$ TMD structure in order to calculate the volume of each NS cavity. MD trajectories were analyzed with the CPPTRAJ program [28] and representative snapshots were obtained using VMD [29]. The root mean squared deviation (RMSD), the time evolution of the distances among selected atoms and the time evolution of angles were monitored over the complete production trajectories. The MM/PBSA.py tool [18] implemented in AMBER was used to compute the electrostatic and van der Waals contributions to the total energy of the molecular mechanics (MM) force field. In this case, the first 20 ns of the holo trajectory were discarded.

Acknowledgments

We thanks to Dr. Dario A. Estrin for useful help with the manuscript. This work was supported by the grants from Agencia Nacional de Promoción Científica y Tecnológica (PICT 2012-2512).

Appendix A. Supplementary data

Supplementary material related to this article can be found, in the online version, at doi:https://doi.org/10.1016/j.jsbmb.2018.04.012.

References

[1] M. Chebib, G.A. Johnston, The 'ABC' of GABA receptors: a brief review, Clin. Exp. Pharmacol. Physiol. 26 (1999) 937–940.

[2] M. Gasior, R.B. Carter, J.M. Witkin, Neuroactive steroids: potential therapeutic use in neurological and psychiatric disorders, Trends Pharmacol. Sci. 20 (1999) 107–112.

[3] D. Belelli, J.J. Lambert, Neurosteroids: endogenous regulators of the GABA(a) receptor, Nat. Rev. Neurosci. 6 (2005) 565–575.

[4] D.S. Reddy, M.A. Rogawski, Neurosteroids - endogenous regulators of seizure susceptibility and role in the treatment of epilepsy, in: J.L. Noebels, M. Avoli, M.A. Rogawski, R.W. Olsen, A.V. Delgado-Escueta (Eds.), Jasper's Basic Mechanisms of the Epilepsies, Bethesda (MD), 2012.

[5] E. Sigel, M.E. Steinmann, Structure, function, and modulation of GABA(a) receptors, J. Biol. Chem. 287 (2012) 40224–40231.

[6] C.J. daCosta, J.E. Baenziger, Gating of pentameric ligand-gated ion channels: structural insights and ambiguities, Structure 21 (2013) 1271–1283.

[7] R. Puthenkalam, M. Hieckel, X. Simeone, C. Suwattanasophon, R.V. Feldbauer, G.F. Ecker, M. Ernst, Structural studies of GABAA receptor binding sites: which experimental structure tells us what? Front. Mol. Neurosci. 9 (2016) 44.

[8] J. Enna, H. Möhler, The GABA Receptors, 3rd edition, Humana Press Inc, 2007.

[9] Z.W. Chen, B. Manion, R.R. Townsend, D.E. Reichert, D.F. Covey, J.H. Steinbach, W. Sieghart, K. Fuchs, A.S. Evers, Neurosteroid analog photolabeling of a site in the third transmembrane domain of the beta3 subunit of the GABA(a) receptor, Mol. Pharmacol. 82 (2012) 408–419.

[10] A.M. Hosie, M.E. Wilkins, H.M. da Silva, T.G. Smart, Endogenous neurosteroids regulate GABAA receptors through two discrete transmembrane sites, Nature 444 (2006) 486–489.

[11] A.M. Hosie, M.E. Wilkins, T.G. Smart, Neurosteroid binding sites on GABA(a) receptors, Pharmacol. Ther. 116 (2007) 7–19.

[12] L.D. Alvarez, D.A. Estrin, Exploring the molecular basis of neurosteroid binding to the beta3 homopentameric GABAA receptor, J. Steroid Biochem. Mol. Biol. 154 (2015) 159–167.

[13] P.S. Miller, A.R. Aricescu, Crystal structure of a human GABAA receptor, Nature 512 (2014) 270–275.

[14] D. Laverty, P. Thomas, M. Field, O.J. Andersen, M.G. Gold, P.C. Biggin, M. Gielen, T.G. Smart, Crystal structures of a GABAA-receptor chimera reveal new endogenous neurosteroid-binding sites, Nat. Struct. Mol. Biol. 24 (2017) 977–985.

[15] P.S. Miller, S. Scott, S. Masiulis, L. De Colibus, E. Pardon, J. Steyaert, A.R. Aricescu, Structural basis for GABAA receptor potentiation by neurosteroids, Nat. Struct. Mol. Biol. 24 (2017) 986–992.

[16] A. Sali, T.L. Blundell, Comparative protein modelling by satisfaction of spatial restraints, J. Mol. Biol. 234 (1993) 779–815.

[17] G.M. Morris, R. Huey, W. Lindstrom, M.F. Sanner, R.K. Belew, D.S. Goodsell, A.J. Olson, AutoDock4 and AutoDockTools4: automated docking with selective receptor flexibility, J. Comput. Chem. 30 (2009) 2785–2791.

[18] B.R. Miller 3rd, T.D. McGee Jr, J.M. Swails, N. Homeyer, H. Gohlke, A.E. Roitberg, MMPBSA.py: an efficient program for end-state Free energy calculations, J. Chem. Theory Comput. 8 (2012) 3314–3321.

[19] J.R. Bracamontes, P. Li, G. Akk, J.H. Steinbach, A neurosteroid potentiation site can be moved among GABAA receptor subunits, J. Physiol. 590 (2012) 5739–5747.

[20] P.A. Davies, E.F. Kirkness, T.G. Hales, Modulation by general anaesthetics of rat GABAA receptors comprised of alpha 1 beta 3 and beta 3 subunits expressed in human embryonic kidney 293 cells, Br. J. Pharmacol. 120 (1997) 899–909.

[21] M.J. Frisch, G.W. Trucks, H.B. Schlegel, G.E. Scuseria, M.A. Robb, J.R. Cheeseman, J.A. Montgomery Jr., T. Vreven, K.N. Kudin, J.C. Burant, J.M. Millam, S.S. Iyengar, J. Tomasi, V. Barone, B. Mennucci, M. Cossi, G. Scalmani, N. Rega, G.A. Petersson, H. Nakatsuji, M. Hada, M. Ehara, K. Toyota, R. Fukuda, J. Hasegawa, M. Ishida, T. Nakajima, Y. Honda, O. Kitao, H. Nakai, M. Klene, X. Li, J.E. Knox, H.P. Hratchian, J.B. Cross, V. Bakken, C. Adamo, J. Jaramillo, R. Gomperts, R.E. Stratmann, O. Yazyev, A.J. Austin, R. Cammi, C. Pomelli, J.W. Ochterski, P.Y. Ayala, K. Morokuma, G.A. Voth, P. Salvador, J.J. Dannenberg, V.G. Zakrzewski, S. Dapprich, A.D. Daniels, M.C. Strain, O. Farkas, D.K. Malick, A.D. Rabuck, K. Raghavachari, J.B. Foresman, J.V. Ortiz, Q. Cui, A.G. Baboul, S. Clifford, J. Cioslowski, B.B. Stefanov, G. Liu, A. Liashenko, P. Piskorz, I. Komaromi, R.L. Martin, D.J. Fox, T. Keith, M.A. Al-Laham, C.Y. Peng, A. Nanayakkara, M. Challacombe, P.M.W. Gill, B. Johnson, W. Chen, M.W. Wong, C. Gonzalez, J.A. Pople, Gaussian 03, Revision C.02, Gaussian, Inc., Wallingford CT, 2004.

[22] D.A. Case, V. Babin, J.T. Berryman, R.M. Betz, Q. Cai, D.S. Cerutti, T.E. Cheatham III, T.A. Darden, R.E. Duke, H. Gohlke, A.W. Goetz, S. Gusarov, N. Homeyer, P. Janowski, J. Kaus, I. Kolossváry, A. Kovalenko, T.S. Lee, S. LeGrand, T. Luchko, R. Luo, B. Madej, K.M. Merz, F. Paesani, D.R. Roe, A. Roitberg, C. Sagui, R. Salomon-Ferrer, G. Seabra, C.L. Simmerling, W. Smith, J. Swails, R.C. Walker, J. Wang, R.M. Wolf, X. Wu, P.A. Kollman, AMBER 14, University of California, San Francisco, 2014.

[23] E.L. Wu, X. Cheng, S. Jo, H. Rui, K.C. Song, E.M. Davila-Contreras, Y. Qi, J. Lee, V. Monje-Galvan, R.M. Venable, J.B. Klauda, W. Im, CHARMM-GUI membrane builder toward realistic biological membrane simulations, J. Comput. Chem. 35 (2014) 1997–2004.

[24] J.A. Maier, C. Martinez, K. Kasavajhala, L. Wickstrom, K.E. Hauser, C. Simmerling, ff14SB: improving the accuracy of protein Side Chain and backbone parameters from ff99SB, J. Chem. Theory Comput. 11 (2015) 3696–3713.

[25] C.J. Dickson, B.D. Madej, A.A. Skjevik, R.M. Betz, K. Teigen, I.R. Gould, R.C. Walker, lipid14: the Amber lipid force Field, J. Chem. Theory Comput. 10 (2014) 865–879.

[26] J. Wang, R.M. Wolf, J.W. Caldwell, P.A. Kollman, D.A. Case, Development and testing of a general amber force field, J. Comput. Chem. 25 (2004) 1157–1174.

[27] P. Schmidtke, V. Le Guilloux, J. Maupetit, P. Tuffery, fpocket: online tools for protein ensemble pocket detection and tracking, Nucleic Acids Res. 38 (2010) W582–589.

[28] D.R. Roe, T.E. Cheatham 3rd, PTRAJ and CPPTRAJ: software for processing and analysis of molecular dynamics trajectory data, J. Chem. Theory Comput. 9 (2013) 3084–3095.

[29] W. Humphrey, A. Dalke, K. Schulten, VMD: visual molecular dynamics, J. Mol. Graph. 14 (33–38) (1996) 27–38.